Anamorphic characterization of a PA-LCoS based holographic data storage system

Francisco J. Martínez-Guardiola, Andrés Márquez, Eva M. Calzado, Roberto Fernández, Cristian Neipp, et al.

Francisco J. Martínez-Guardiola, Andrés Márquez, Eva M. Calzado, Roberto Fernández, Cristian Neipp, Manuel Ortuño, Inmaculada Pascual, Sergi Gallego, "Anamorphic characterization of a PA-LCoS based holographic data storage system," Proc. SPIE 10751, Optics and Photonics for Information Processing XII, 1075112 (7 September 2018); doi: 10.1117/12.2321276

SPIE.

Event: SPIE Optical Engineering + Applications, 2018, San Diego, California, United States

Anamorphic characterization of a PA-LCoS based holographic data storage system

Francisco J. Martínez-Guardiola[1,2,*], Andrés Márquez[1,2], Eva M. Calzado[1,2], Roberto Fernández[1,2], Cristian Neipp[1,2], Manuel Ortuño[1,2], Inmaculada Pascual[2,3], Sergi Gallego[1,2]

[1]Dept. de Física, Ing. de Sistemas y Teoría de la Señal, Universidad de Alicante, P.O. Box 99, E-03080, Alicante, Spain; [2]I.U. Física Aplicada a las Ciencias y las Tecnologías Universidad de Alicante, P.O. Box 99, E-03080, Alicante, Spain; [3]Dept. de Óptica, Farmacología y Anatomía, Universidad de Alicante, P.O. Box 99, E-03080, Alicante, Spain

*fj.martinez@ua.es; phone (+34) 965-903-692

ABSTRACT

We have included a Parallel Aligned Liquid Crystal on Silicon (PA-LCoS) microdisplay in a Holographic Data Storage System (HDSS). This novel display, widely accepted as Spatial Light Modulator (SLM), presents some advantages and disadvantages. One of these disadvantages is the anamorphic and frequency dependent effect. In this work we want to test this effect and see its effects in the complete optical process involved in the HDSS. We will use stripe-based patterns with different orientation (vertical and horizontal). To check the limits, we will increase the data density by decreasing the minimum stripe width. For evaluating the degradation suffered by the data page, we use the Bit Error Rate (BER) as figure of merit. We make a BER calculation from the statistical analysis of the histogram. In addition to the anamorphic effects we evaluate the degradation effects introduced by the non-uniformity in the illumination. To this goal we divide the image in several regions that are processed in the same way that the entire image. The error analysis of the entire optical system is useful for its calibration and fine adjustment. Once we have characterized the experimental setup we introduce the holographic material. Thus, by making the same analysis, we can evaluate the errors introduced by the material. As holographic material we use Polyvinyl Alcohol Acrylamide (PVA/AA), that has been characterized and developed in previous works by our group.

Keywords: Liquid-crystal devices, Parallel-aligned, Holographic optical elements, Spatial light modulators, Optical processing, Holographic and volume memories.

1. INTRODUCTION

As long as we are developing a Holographic Data Storage System (HDSS), we have to face some technological problems[1,2]. In our HDSS we have used a PA-LCoS microdisplay as a data pager[3]. We have introduced it because we are interested in phase multilevel modulation schemes[4]. In this work we develop a characterization method that allows us to predict the performance by evaluating the limitations introduced by the elements in our optical system.

In previous works, we have detected that due to the digital addressing technology used in the PA-LCoS microdisplay introduces some degradation effects as flicker in the retardance response, and we have done an intense work characterizing it[5]. Other degradation phenomena such as fringing field, anamorphic and frequency dependent effects have been detected[6]. In this work we want to focus on analyzing the anamorphic effect[6] in our PA-LCoS data pager. We want to know if it is an important element that affects our storage capability. The anamorphic effect is related with the device electronic drivers, in which the signal that forms the image is structured by rows that are addressed pixel by pixel, so the horizontal frequency is much larger than the vertical frequency. This provokes a low-pass filtering in the signal that affects differently the vertical or horizontal variations in the image. Anamorphic and frequency dependent effects may also be due to other phenomena such as fringing-field or LC adherence in the transverse direction between neighbouring LC molecules.

As long as we want to focus on identifying if the anamorphic and frequency dependent phenomenon affects our HDSS, in a first place, we will need to evaluate the maximum resolution of the complete optical system. We will see how we

Optics and Photonics for Information Processing XII, edited by Abdul A. S. Awwal, Khan M. Iftekharuddin, Mireya García Vázquez, Andrés Marquez, Víctor H. Diaz-Ramirez Proc. of SPIE Vol. 10751, 1075112 · © 2018 SPIE · CCC code: 0277-786X/18/$18 · doi: 10.1117/12.2321276

can obtain information about the illumination, so we also present a local characterization to these no-uniformities of the illumination[6].

To allow a quantitative evaluation on these issues, and because we consider a binary data storage system, we use as figure of merit the Bit Error Rate (BER) or the Quality factor (Q-factor). We analyze the errors encountered in the image retrieved by a CCD camera.

We will also study how the introduction of the recording material affects the performance of the system. In this way we assure that the complete HDSS is tested.

2. EXPERIMENTAL SETUP

Our HDSS uses a convergent correlator architecture for the object beam[7]. This setup provides us some flexibility. We do not have the selecting restriction that a 4-f system constrains, and we can vary the areal density on the recording material without changing any setup lens[8].

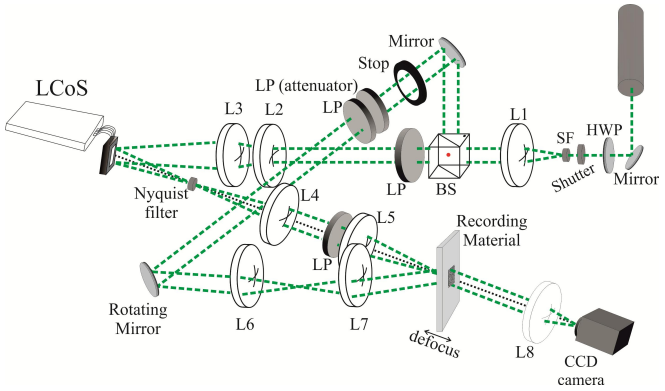

Figure 1. Scheme of our experimental setup using convergent correlator and PA-LCoS as a Data Pager.

Figure 1 shows the complete HDSS developed. The beam splitter (BS in Fig.1) divides the object beam from the reference beam, the object beam follows the path formed by lenses L2 to L5, as can be seen the PA-LCoS is in this path to introduce the data. Reference beam follows the path formed by lenses L6 and L7. As long as we are interested in the retrieved data that has been introduced by the PA-LCoS, we will work on the object beam combined with the lens L8. The combination of L2 and L3 enables to modify the convergence angle of the beam onto the LCoS. The beam impinges onto the display while it is converging. At the convergence plane, where the Fourier Transform in formed, we place a Nyquist filter that allows us to control the number of orders that it will be stored. But in this work, we do not make use, or cut any order, because we are interested in the limitations of the entire setup. Lenses L4 and L5 from a relay system to image the Nyquist filter plane, which contains the binary information, onto the recording plane. The incident angle to separate impinging and reflecting object beam is 11.5º, and it is fixed during all the experiment.

The PA-LCoS used in our setup is a commercially available PA-LCoS microdisplay, model PLUTO distributed by the company HOLOEYE. It is filled with a nematic liquid crystal, with 1920x1080 pixels and 0.7" diagonal. The fill factor is 87% and its pixel pitch is 0.8μm.

The pixel pitch will define the information bit size for different resolutions. We will use different patterns to analyze the performance of our system. We vary the number of pixels used in the PA-LCoS to represent a bit of information. This bit sizes are 8x8, 4x4, 3x3, and 2x2 pixels in the display. So, we have formed square bits with, 64μm, 32μm, 24μm and 16μm side length. As long as we will arrange this bits of information in stripes, theses side length will define the minimum stripe width. Therefore, for statistical reasons, we will also use square bits to calculate the BER. We make use of data pages formed by 512x512 pixels in the PLUTO display. If we would consider stripes as a block of information, we would only have 64 information blocks for 8x8 pixel size, 128 for 4x4 and so on. This numbers are insufficient for a statistical analysis, so considering individual bits we will have 4096 bits of information for a 8x8 pixel size image, 16384 for 4x4, etc.

For retrieving information we use a CCD camera, specifically the PCO.1600 model from PCO.imaging manufacturer. This is a high dynamic 14 bits cooled CCD camera with a resolution of 1600x1200 pixels, and a pixel size of 7.4x7.4μm^2. The magnification of the PA-LCoS plane onto the camera plane is about a factor of two. So, we can consider that do not exist limitation in the image retrieving, by the CCD camera, since the image is oversampled.

3. CHARACTERIZATION METHOD

The first limitation that we have to analyze is the one produced by the aperture of the lenses. We need to test the resolution capability of our HDSS. To obtain the resolving power of the complete optical system, composed by lenses L4, L5 and L8 (see Fig. 1), we use a standard 1951 USAF test target. To do that we replace the PA-LCoS screen by a negative 1951 USAF resolution test chart, and we capture the reflected image with the CCD camera. In this case, reference beam are blocked to avoid problems and we do not introduce any recording material in the object beam path.

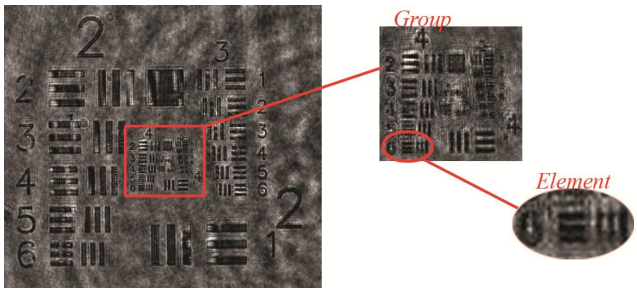

Figure 2. Retrieved image from the negative USAF pattern used to test the resolution capability.

Figure 2 shows the retrieved image of the 1951 USAF resolution test target. From this image, we conclude that we can distinguish Group 4 Element 6, which corresponds to a resolution of 28.50 lp/mm or 35.09μm per line pair. So the maximum line width that we can resolve will be 17.54μm. If we translate this data into the patterns that we have prepared we obtain that the stripe formed by two pixels in the PA-LCoS (8+8=16μm) cannot be resolved. This will limit the patterns that we can use as they were presented in the previous section.

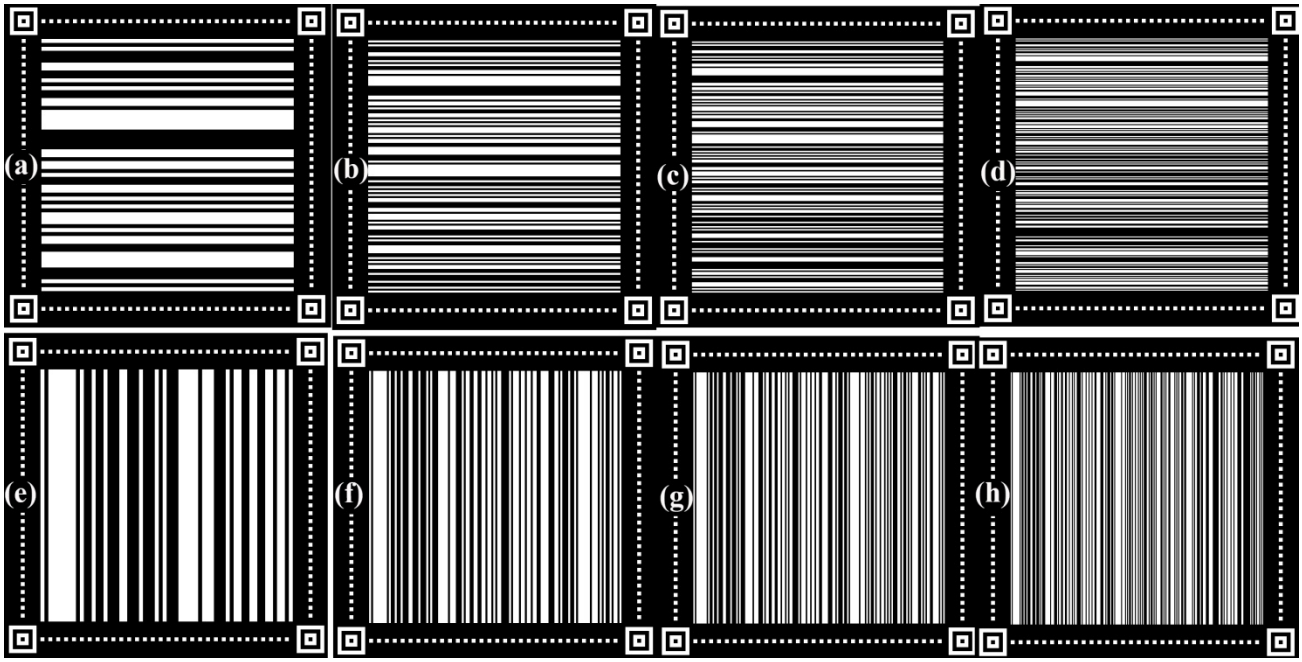

Figure 3. Patterns used for characterizing anamorphic effect. (a) Horizontal Stripe width of 8 pixels (b) Horizontal Stripe width of 4 pixels (c) Horizontal Stripe width of 3 pixels (d) Horizontal Stripe width of 2 pixels (e) Vertical Stripe with of 8 pixels (f) Vertical Stripe with of 4 pixels (g) Vertical Stripe with of 3 pixels (h) Vertical Stripe with of 2 pixels

To test the well known anamorphic effects presented by this kind of microdisplays[9-11], we have prepared a set of test patterns with different resolutions and with two orientation, vertical and horizontal.

When we talk about different resolution we refer to the number of pixels that form a bit of information. In Figure 3 we can see the patterns designed: all the patterns showed in Fig. 3 are formed by 512x512 pixels in the PA-LCoS (without taking into account the fiducial marks). Using these 512x512 pixels we have to form a pattern with different resolutions, so we use a set of pixels to define a bit of information. For example, in Fig. 3 (a) we are using 8x8 pixels in the display to represent a bit, so we can form a pattern with 64x64 bits of information, in our case, as we are interested in anamorphic effect, we distribute the bits in stripes, so Fig. 3(a) is the pattern that corresponds to a stripe width of 8 pixels and for the horizontal orientation. Fig 3 (e) correspond to the same resolution (8x8pixel/bit) but the other orientation (vertical). Fig. 3 (b), (c) and (d) corresponds to horizontal orientation and resolutions of 4x4pixel/bit, 3x3 pixel/bit and 2x2 pixel/bit, respectively. Fig. 3 (f), (g) and (h) corresponds to vertical orientation and resolutions of 4x4pixel/bit, 3x3 pixel/bit and 2x2 pixel/bit, respectively. The stripes are generated randomly to avoid diffraction effects, and for the patterns always start with a white stripe followed by a black stripe and finish with a black stripe followed by a white stripe. In the case of horizontal orientation the sequence order is from top to bottom and in the case of the vertical orientation the order is from left to right. The fiducial marks are added for centering and rotation, and with the purpose of detecting the position of the information bits. These marks can also serve us to evaluate the quality of the image or distortion introduced during the image capture. The width of the lines composing the fiducial marks is maintained constant and they are always formed by 8 pixels.

In this work, and for simplicity, we have used a Binary Intensity Modulation (BIM) scheme[4]. We configured the PA-LCoS with an electrical configuration that offers a 180º retardance range, with good linearity, and allow us to obtain the maximum contrast and the less flicker possible, as we analyzed in [12]. The maximum contrast will be produced when the linear polarizers (LP) used in the object beam (see Fig. 1) are crossed with respect to each other, forming a 45º angle with respect the neutral lines of our PA-LCoS display.

Our characterization method is applied in two phases. In a first place we illuminate the PA-LCoS and we produce the image of the data page onto the CCD camera with the help of L4, L5 and L8 lenses (see Fig. 1)[8]. The image data obtained is then digitally analyzed. In this phase we do not introduce recording material in its corresponding plane. This will give us information about how the optical setup is affecting the BER, and it will establish our starting point for comparing, in a second phase, with the data that will be obtained when we insert a recording material.

The first step that we have to do is to convert the captured image, which is in a gray scale, in to a binary image. To do that, we have to select the best threshold value to separate the 0 level from the 1 level. In this step we select the threshold value that minimizes the number of errors when we compare the thresholded image with the original one. To calculate the number of errors and therefore the BER we compare at a bit level. That means that we consider the image data as a grid that will depend on the resolution selected. For an 8x8 bit size we have 64x64 (4096) bits of information, for a 4x4 bit size we have 128x128 (16384) bits, and so on.

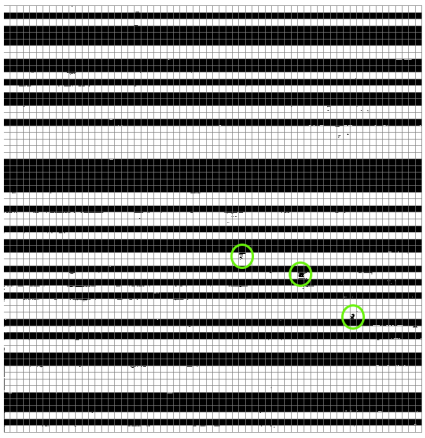

Figure 4. Thresholded image with a grid that indicates the position of the information bits. Bit size 8x8 pixels. Possible detected errors are marked in green.

In Fig. 4 we show a thresholded image captured for a horizontal orientation and an 8x8pixels bit size. As we know the position of the 0's and 1's we can make a simple count of how many bits we have detected wrongly. In Fig. 4 we have marked in green 3 possible mistakenly detected bits. From this count we can calculate the BER just by dividing for the total number of bit (in this case 4096). But as we can detect the position of every bit and its original value, we can construct a histogram of the non-processed captured image by counting the number of bits for every gray level and classified as 0's or 1's respectively.

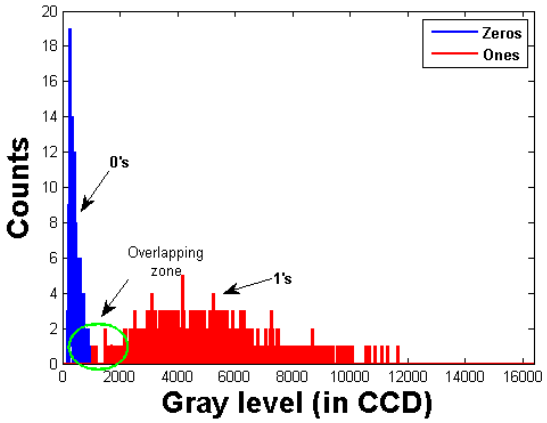

Figure 5. Histogram of 0's and 1's from an non-processed (no-thresholded) captured image.

In Fig.5 we can see the calculated histogram for a non-processed image with the corresponded ON and OFF levels marked (1's and 0's). This figure is important because we can make some statistical calculation to obtain a more robust value for the BER. In Fig. 4 the calculated BER can be distorted by an statistical fluctuation that can make us to detect less errors and this fact can change our resulting appreciation of the BER. From Fig. 5 we can also evaluate the image quality by observing the "Overlapping zone" marked, this zone is where the bits can be interpreted wrongly, and it will be the range of gray level that define the best threshold level to binarize the image. For this reason, if we observed a well separated histogram we can predict a good value for the BER, in the other way, if this overlapping zone is bigger we can predict a higher BER. From this histogram we can calculate the Q-factor typically used in digital systems in bier optics communications[13-15]. Q factor is given by:

$$Q = \frac{|\mu_1 - \mu_0|}{\sigma_1 + \sigma_0}, \tag{1}$$

where μ_1 and μ_0 are the mean value in the histograms produced for the gray level distribution of 1's (ON) and 0's (OFF) bits respectively, and σ_1 and σ_0 are the corresponding standard deviations. If the histograms are approximated as Gaussian distributions, the relation between BER and Q-factor is given by,

$$BER = \frac{1}{2}\left[1 - erf\left(\frac{Q}{\sqrt{2}}\right)\right], \tag{2}$$

Where *erf* is the error function[13-15], which is tabulated in various mathematical handbooks[16,17]. With this values (Q-factor and BER) we can predict the capacity of the optical system to recover the digital information stored. We need a raw BER in the range of 10^{-3} to assure a complete information recovery after introducing error correction codes[13-15]. In this work we are evaluating the raw BER, we do not make use of any error correction codes.

4. EXPERIMENTAL RESULTS

In this section we present the results obtained for the image captured. As mentioned in the previous section we use image formed by stripes of bits oriented vertically or horizontally to test the anamorphic effects. We use different bit size, or

resolutions, and we test how the introduction of recording material affects the performance of our system. The figure of merit to evaluate the quality of the output in our system will be the BER and Q-factor.

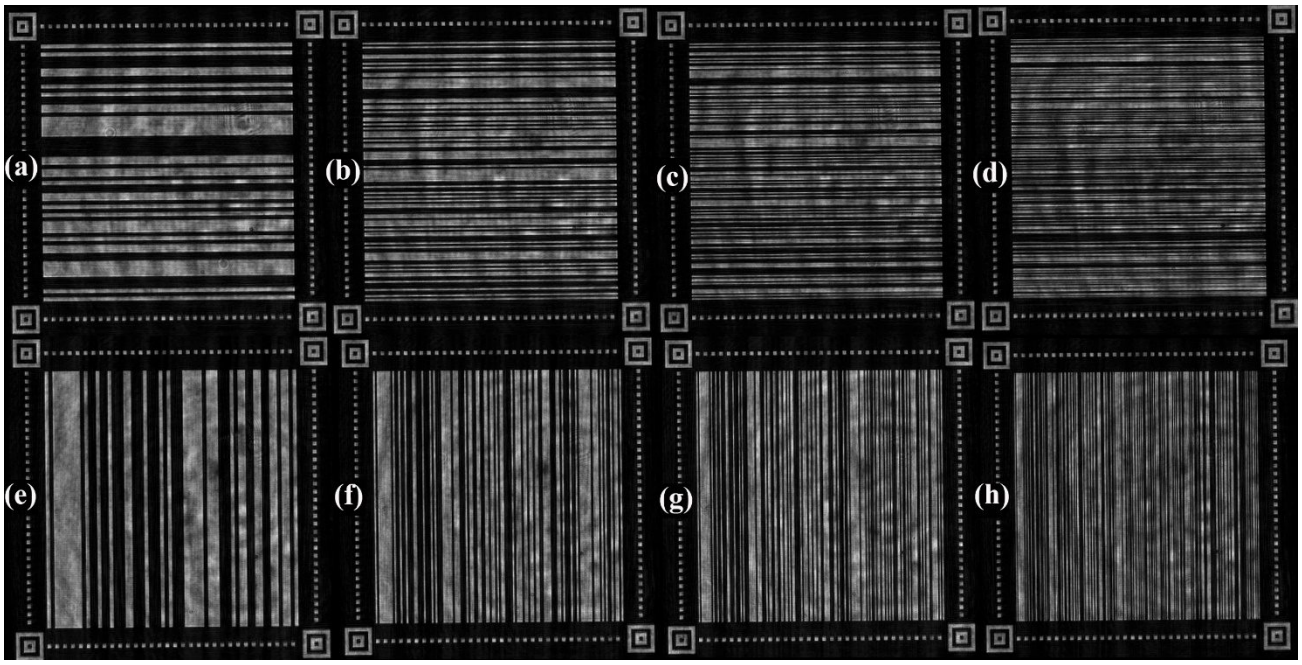

Figure 6. Images captured by CCD camera. (a) Horizontal Stripe width of 8 pixels (b) Horizontal Stripe width of 4 pixels (c) Horizontal Stripe width of 3 pixels (d) Horizontal Stripe width of 2 pixels (e) Vertical Stripe with of 8 pixels (f) Vertical Stripe with of 4 pixels (g) Vertical Stripe with of 3 pixels (h) Vertical Stripe with of 2 pixels

In Fig. 6 we can see the images captured by our CCD camera, it has a bit depth of 14 bits, so we have 16384 possible gray levels. As long as we avoid saturating the CCD, we do not need to consider a full variation of levels to seek for the best threshold level. At this level, the number of counted errors would be the minimum.

Table 1. Bit error rate and Q-factor for Horizontal stripes

Bit size	Q-factor	Errors	BER
8x8	3.082	1	$1.0\ 10^{-3}$
4x4	2.473	25	$6.8\ 10^{-3}$
3x3	2.243	117	$12.5\ 10^{-3}$
2x2	0.574	18097	$2.8\ 10^{-1}$

Table 2. Bit error rate and Q-factor for Vertical stripes

Bit size	Q-factor	Errors	BER
8x8	3.124	3	$9.0\ 10^{-4}$
4x4	2.884	8	$2.0\ 10^{-3}$
3x3	2.650	26	$4.0\ 10^{-3}$
2x2	1.699	2371	$4.5\ 10^{-2}$

In Table 1 and Table 2 we show the calculated Q-factor, BER and the number of errors for the best threshold level for Horizontal and Vertical stripes respectively. Q-factor and BER are calculated from the histograms of the images in Fig. 6 and using equation (1) and (2). We show how the BER is maintained in the level required for an appropriate recovery. As we predict in the previous section, by using the 1951 USAF resolution test target, for the bit size formed with 2x2 pixel in the LCoS we do not have enough resolution in our optical system to form an appropriate image, so the BER and the minimum number of errors are increased abruptly. We can also observe that the Q-factor and BER values are better for the vertical stripes images. This contradicts the results in diffractive optical elements displayed on LCoS devices [8,10,11] where diffraction efficiency becomes smaller for vertically oriented elements. An explanation for this can came from a wider tolerance to the anamorphic effect when a LCoS device is used in a HDSS using a BIM scheme, and now we are not displaying periodic elements and the figure of merit is not diffraction efficiency. In this case, the binary intensity contrast between ON and OFF levels is the key magnitude and this has a limited dependency with the orientation of the no-periodic stripes used in our present application.

To analyze the illumination inhomogeneities we have divided the image in four zones. In this way, each of them can be analyzed as we have done with the full image. We will obtain the same figure of merit but for different localizations in the image.

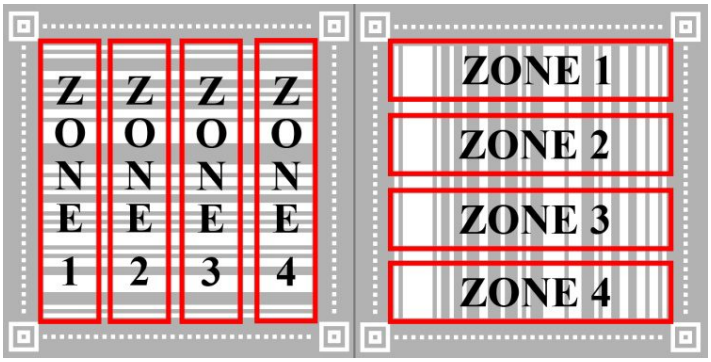

Figure 7. Zones defined for illumination homogeneity analysis.

In Fig. 7 we see how we have defined the zones for the local characterization of the illumination. The zones always have the same distribution independently of the resolution used. In this way we assure that for low resolutions (8x8) we still have enough data in all zones to make a statistical analysis. So, we can extract data from the different zones, in order to detect possible illumination problems.

Table 3. Measured Q-factor (**BER**) by zone and for Horizontal stripes

Full image	*Zone 1*	*Zone 2*	*Zone 3*	*Zone 4*
		8x8 pixels bit size		
3.082(**1.0 10^{-3}**)	3.266(**5.5 10^{-4}**)	3.185(**7.2 10^{-4}**)	2.977(**1.5 10^{-3}**)	3.110(**9.4 10^{-4}**)
		4x4 pixels bit size		
2.473(**6.8 10^{-3}**)	2.516(**5.9 10^{-3}**)	2.648(**4 10^{-3}**)	2.411(**8.0 10^{-3}**)	2.462(**6.9 10^{-3}**)
		3x3 pixels bit size		
2.243(**12.5 10^{-3}**)	2.226(**13.0 10^{-3}**)	2.354(**9.3 10^{-3}**)	2.202(**13.8 10^{-3}**)	2.297(**10.8 10^{-3}**)

In Table 3 we can see the results obtained for the Q-factor and BER (inside parenthesis) for all the resolutions used and for the zones defined in Fig. 7. In this case we see how the worst results are related with zone 3 and zone 4 for all the resolutions. That means that the right part of the image is worst illuminated, or we have some problem with these local zones. Analyzing the pictures in Fig. 6 (a,b,c,d) is hard to say where we will obtain worst results. The resolution that corresponds to the 2x2 pixel size bit has not been considered because as we saw is out of the optical limit of our system, and it could lead us to misleading conclusions.

Table 4. Measured Q-factor (**BER**) by zone and for Vertical stripes

Full image	*Zone 1*	*Zone 2*	*Zone 3*	*Zone 4*
		8x8 pixels bit size		
3.124(**9.0 10^{-4}**)	3.558(**1.9 10^{-4}**)	3.439(**2.9 10^{-4}**)	2.955(**1.4 10^{-3}**)	2.909(**1.8 10^{-3}**)
		4x4 pixels bit size		
2.884(**2.0 10^{-3}**)	3.195(**7.0 10^{-4}**)	3.012(**1.3 10^{-3}**)	2.790(**2.6 10^{-3}**)	2.685(**3.6 10^{-3}**)
		3x3 pixels bit size		
2.650(**4.0 10^{-3}**)	2.668(**3.8 10^{-3}**)	2.586(**4.9 10^{-3}**)	2.747(**3.0 10^{-3}**)	2.671(**3.8 10^{-3}**)

In Table 4 we see the results obtained for vertical orientation and different zones. Again, the worst results correspond to the zone 3 and 4. So we are referring, according to Fig. 7, to the bottom part of the image. Combining Table 3 and 4 we can say that the bottom right sector of the image are worst illuminated that the other, in this way we can focus on improving our setup to avoid this effect.

As we had said, if we want to maintain the possibility for performing a statistical analysis, we can not reduce the zones of our data. Nevertheless, as a qualitative evaluation we have calculated the number of errors for every column (if we are using horizontal stripes) or for every row (if we are using vertical stripes).

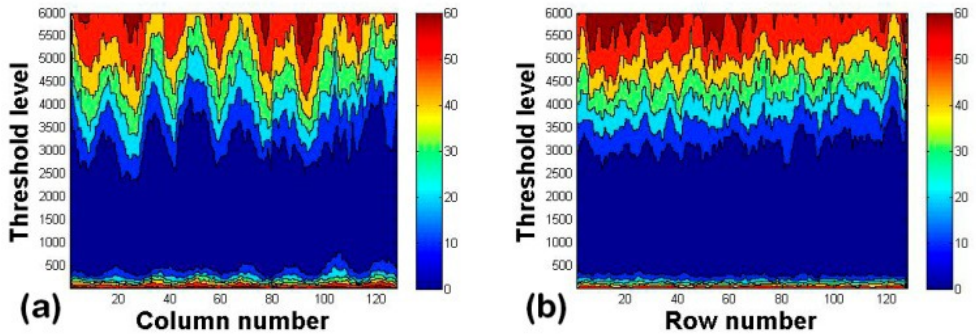

Figure 8. Number of errors committed as a function of threshold level: (a) for each column (Horizontal Stripes) (b) for each row (Vertical Stripes). Data page resolution 4x4 pixels per bit.

In Fig. 8 we have represented the number or errors as a function of the threshold level and for every column (for Horizontal Stripes) or for every row (for Vertical stripes). This kind of graphs allow us to evaluate the illumination and the influence of the threshold in the errors counted. In Fig. 8 we appreciate a wide blue zone that indicates a good separation between ON and OFF levels, the graph also reflects a ripple in Fig. 8 (a) that corresponds to the horizontal orientation that it is the orientation with a worse result in BER, maybe this is a clue about how the illumination inhomogeneities affects to the results depending on the orientation.

Until now, we have analyzed the performance of our HDSS without introducing the material, this is our starting point for comparing with the result when we store the data in a photopolymer and we reconstruct them. When we introduce the photopolymer, new sources of distortion appears. We use a Polyvinyl Alcohol Acrylamide (PVA/AA) photopolymer developed and manufactured by our group[18]. During the manufacturing process, ripples on the surface can be introduced and deformations due to continuous exchange of water molecules with the environment, as well as the natural crystallization process may affect the recording process[18].

We apply the same method exposed, which means that we capture the image with the CCD camera and we obtain the histogram and with the help of eq. (1) and (2) we calculate the Q-factor and BER. We only present here the results for a 8x8 pixel per bit size resolution and 4x4 pixel per bit size resolution, since as we will see the degradation prevents getting results for smaller resolutions.

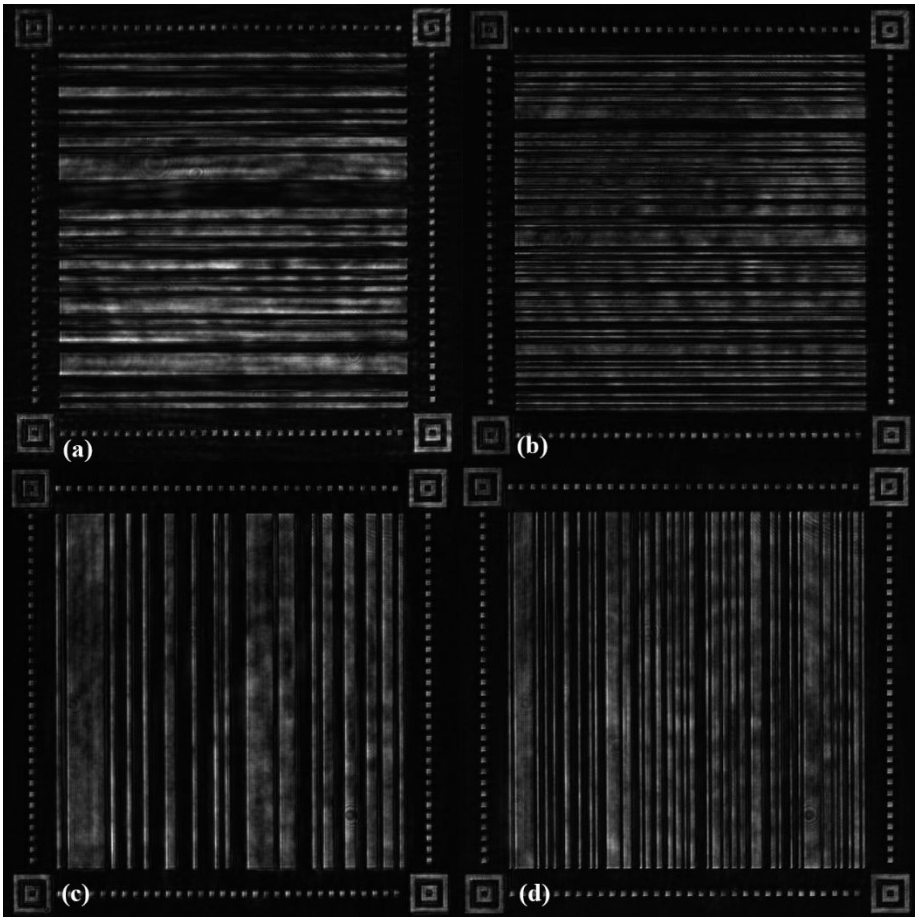

Figure 9. Reconstructed images for: (a) 8x8 pixels/bit Horizontal (b) 4x4 pixels/bit Horizontal (c) 8x8 pixels/bit Vertical (d) 4x4 pixels/bit Vertical

In Fig. 9 se show the reconstructed images captured by the CCD during the reconstruction process, notice that for reconstruction we are making use of the reference beam, so all the HDSS setup has tested. With the naked eye we can see that the images are degraded, so we expect an increasing in the BER, and a decreasing in the Q-factor.

Table 5. BER and Q-factor for Horizontal stripes in the reconstructed images

Pixel size	Q-factor	Errors	BER
8x8	1.995	46	$23\ 10^{-3}$
4x4	1.514	850	$65\ 10^{-3}$

Table 6. BER and Q-factor for Vertical stripes in the reconstructed images

Pixel size	Q-factor	Errors	BER
8x8	1.687	109	$46\ 10^{-3}$
4x4	1.663	486	$48\ 10^{-3}$

In Table 5 and 6, we can observe how the Q-factor and BER change when the material is introduced. If we compare with the corresponding results presented in Table 1 and 2, we see that the number of errors increases by one order of magnitude. The resolutions under a bit size of 4x4 pixels are out of the values that can be recovered with an error correction code. This can be produced by the non-uniformity in the illumination that affects the registration process, and the slight non-uniformity in the deposition of the material has a relevant role in the reduction of the performance.

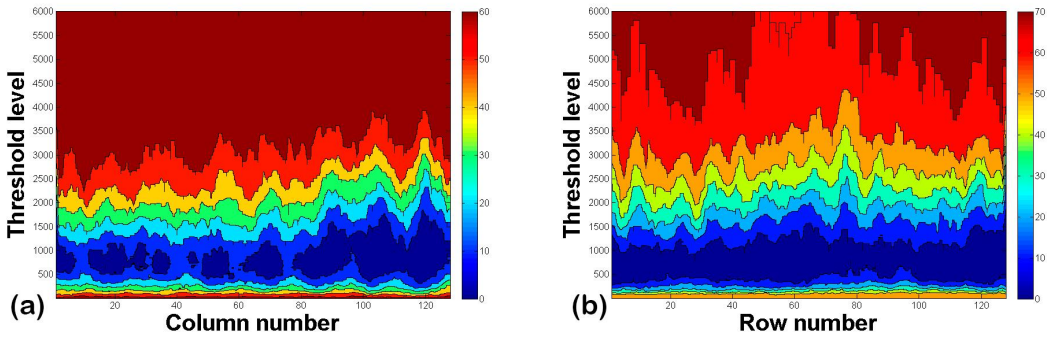

Figure 10. Number of errors committed as a function of threshold level when material is introduced: (a) for each column (Horizontal Stripes) (b) for each row (Vertical Stripes). Data page resolution 4x4 pixels per bit.

In Fig. 10 we want to show how the degradation of the reconstructed image can be observed using the tools developed with this method. We can compare Fig. 10 which is the same showed in Fig. 8 but with material. Fig. 10 corresponds to the data showed in Table 5 and 6, and Fig. 8 corresponds to the data showed in Table 1 and 2. We see how the blue region has been narrowed, so the election of the threshold level would be crucial, and the fact that the blue region is narrowed also give us a clue about how the image is degraded and with less contrast as we can confirm comparing Fig. 9 and Fig. 6.

5. CONCLUSIONS

We have developed a systematic method to test the limits of a Holographic Data Storage System[6], that takes into account the existence of anamorphic an frequency dependent effects due to the signal addressing system that drives the modern digital microdisplays as the PA-LCoS used. To do that we defined two figures of merit, the Q-factor and BER.

We have seen that the anamorphic effect does not play an important role in the degradation when non-periodic patterns are used. This effect seems to have an influence when we use periodic diffractive optical elements as we noticed in previous works[5]. The fact that the BER is in the order of 10^{-3} or below, even with a resolution of 3x3 pixels per bit, shows that we can reconstruct data pages in a reliable way.

The graphs and data that we can obtain from the data analysis allow us to predict illumination problems, dividing the image in four zones permit us to characterize the illumination locally.

We have seen how affect the introduction of the holographic material, and the BER is still good enough to consider that the data can be recovered. But we have to make an effort to improve the material homogeneity during the manufacturing process.

ACKNOWLEDGEMENTS

This work was supported by Ministerio de Economía, Industria y Competitividad (Spain) under projects FIS2017-82919-R (MINECO/AEI/FEDER, UE) and FIS2015-66570-P (MINECO/FEDER), by Generalitat Valenciana (Spain) under project PROMETEO II/2015/015 and by Universidad de Alicante under project GRE17-06.

REFERENCES

[1] H. J. Coufal, D. Psaltis, and B. T. Sincerbox, eds, "Holographic Data Storage", Springer-Verlag, New York (2000)
[2] K. Curtis, L. Dhar, A. Hill, W. Wilson, M. Ayres, eds., "Holographic Data Storage: From Theory to Practical Systems", John Wiley & Sons, Ltd., Chichester, (2010)
[3] G. Lazarev, A. Hermerschmidt, S. Kruger, S. Osten, "LCoS spatial light modulators: trends and applications", in Optical Imaging and Metrology: Advanced Technologies, W. Osten and N. Reingand eds., Wiley-VCH Verlag & Co., Weinheim (2012)

[4] F. J. Martínez, R. Fernández, A. Márquez, S. Gallego, M. L. Álvarez, I. Pascual, A. Beléndez, "Exploring binary and ternary modulations on a PA-LCoS device for holographic data storage in a PVA/AA photopolymer", Opt. Express, 23(16), 20460-20479 (2015)
[5] F. J. Martínez, A. Márquez, S. Gallego, M. Ortuño, J. Francés, I. Pascual and A. Beléndez "Predictive capability of average Stokes polarimetry for simulation of phase multilevel elements onto LCoS devices" Appl. Opt., 54, no. 6, 1379-1386 (2015)
[6] F. J. Martínez-Guardiola, A. Márquez, E. M. Calzado, S. Bleda, S. Gallego, I. Pascual and A. Beléndez "Anamorphic and Local Characterization of a Holographic Data Storage System with a Liquid-Crystal on Silicon Microdisplay as Data Pager", Appl. Sci., 8, 986 (2018)
[7] A. VanderLugt [Optical Signal Processing], John Wiley & Sons, (1992)
[8] A. Márquez, E. Fernández, F. J. Martínez, S. Gallego, M. Ortuño, A. Beléndez, I. Pascual "Analysis of the geometry of a holographic memory setup" Proc. SPIE, 8429, 84291Y (2012)
[9] L. Lobato, A. Lizana, A. Márquez, I. Moreno, C. Iemmi, J. Campos, and M. J. Yzuel, "Characterization of the anamorphic and spatial frequency dependent phenomenon in liquid crystal on silicon displays" J. Eur. Opt. Soc. Rapid Pub., 6, 11012S (2011)
[10] J. Albero, P. García-Martínez, J. L. Martínez, and I. Moreno, "Second order diffractive optical elements in a spatial light modulator with large phase dynamic range," Opt. Lasers Eng., 51, 111–115 (2013)
[11] M. Wang, F. J. Martínez, A. Márquez, Y. Ye, L. Zong, I. Pascual, and A. Beléndez, "Polarimetric and diffractive evaluation of 3.74 micron pixel-size LCoS in the telecommunications C-band," Proc. SPIE, 10395, 103951J (2017)
[12] F. J. Martínez, A. Márquez, S. Gallego, M. Ortuño, J. Francés, A. Beléndez, I. Pascual, "Electrical dependencies of optical modulation capabilities in digitally addressed parallel aligned liquid crystal on silicon devices," Opt. Eng., 53(6), (2014)
[13] L. Ramamoorthy, V. K. Kumar, A. Hoskins, K. Curtis, "Data Channel Modeling," Chapter 10. Holographic Data Storage: from Theory to Practical systems" John Wiley & Sons, Ltd. Chichester, 221-245 (2010
[14] G. P. Agrawal [Fiber-Optic Communication Systems], John Wiley & Sons, (2010)
[15] G. Keiser, [Optical Fiber Communications], McGraw-Hill, 4th ed., New York, (2011)
[16] W. Navidi, [Principles of Statistics for Engineers and Scientists], McGraw-Hill, New York, (2010)
[17] D. Zwillinger, ed., [Standard Mathematical Tables and Formulae], CRC Press, Florida, 31st ed. (2003)
[18] M. Ortuño, S. Gallego, C. García, C. Neipp, A. Beléndez, I. Pascual "Optimization of a 1mm thick PVA/acrylamide recording material to obtain holographic memories: method of preparation and holographic properties" Appl. Phys. B, 76:851 (2003)